THE ASTROPHYSICAL JOURNAL, 414:L9–L12, 1993 September 1


# ULTRAVIOLET PHOTOMETRY OF OB ASSOCIATIONS IN M31

JESSE K. HILL,[1] JOAN E. ISENSEE,[1] RALPH C. BOHLIN,[2] ROBERT W. O'CONNELL,[3] MORTON S. ROBERTS,[4]
ANDREW M. SMITH,[5] AND THEODORE P. STECHER[5]
*Received 1993 March 23; accepted 1993 June 10*

## ABSTRACT

Near-UV (2490 Å) and far-UV (1520 Å) magnitudes are obtained for 76 massive stars in 24 OB associations in the central and southern portions of M31 from images obtained by the Ultraviolet Imaging Telescope during the *Astro 1* spacelab mission. UV photometry is important because the most massive stars are brightest in the UV, the sensitivity to interstellar extinction is largest there, and because stars detected in the far-UV are unlikely to be foreground Galactic stars. A comparison is made with the previous UIT photometry of 30 stars in the giant association NGC 206 (A78). The brightest stars in the far-UV band in NGC 206 are $\sim 1$ mag brighter than the brightest stars in any of the other associations. The most likely explanation for the brighter stars in NGC 206 is the lower extinction, together with more recent formation of at least some massive stars. Extinctions are estimated from the relation between $E(B-V)$ and the distance from the center of M31 derived by Hodge and Lee from optical CCD stellar photometry, although the extinction of NGC 206 is assumed to follow the reddening model of Hutchings, Bianchi, and Massey. From evolutionary models we estimate lower limits to the maximum stellar mass at $\sim 60$–$100\ M_\odot$ in NGC 206, A29, A61, A63, A130, and A132. For other associations, the limits are in the range $\sim 20$–$55\ M_\odot$. The association with the most measured stars other than NGC 206 is A21, with 15. The brightest star in A21 is 2 mag fainter than the brightest star in NGC 206 with mass $\sim 40\ M_\odot$, if it is a supergiant at the age of maximum far-UV luminosity. The faintness of the stars in A21 is only partially accounted for by increased extinction, according to the relation of Hodge and Lee. Ages are estimated at 3–11 Myr for the most recent star formation in each association, if the star with the brightest $m_{152}$ magnitude is a blue supergiant. A mass range is computed for the brightest star in the far-UV band by assuming that it is either on the zero-age main sequence (maximum mass) or a supergiant with maximum far-UV luminosity (minimum mass).

*Subject headings:* galaxies: general — galaxies: individual (M31) — ultraviolet: galaxies

## 1. INTRODUCTION

Regions of active or recent star formation, where the emission is dominated by luminous hot massive stars, are prominent on ultraviolet images of spiral galaxies (e.g., Hill, Bohlin, & Stecher 1984; Bohlin et al. 1990; Hill et al. 1992a, b). Stars detected in the far-UV band have a much lower likelihood of being chance superpositions of intrinsically fainter foreground stars than stars detected in optical bands. Far-UV (1520 Å) and near-UV (2490 Å) images of the central and southern parts of the local group Sb galaxy M31 were obtained by the Ultraviolet Imaging Telescope during the 1990 December *Astro 1* spacelab mission. Near-UV and far-UV photometry of 30 stars in the OB association NGC 206 were reported by Hill et al. (1992b). In this *Letter* we compare UV photometry of 76 stars in 24 additional OB associations in M31 (van den Bergh 1964) with the previous UIT photometry of NGC 206 (A78).

Although ground-based color-magnitude diagrams in optical bands from CCD images have been published for about a dozen M31 associations (e.g., Massey, Armandroff, & Conti 1986; Hodge & Lee 1988; Hodge et al. 1987), UIT data enable a substantial increase in our knowledge of the most massive stars in M31. A future publication (Hill et al. 1993) will give positions and UV magnitudes for over 500 stars in 37 M31 associations, together with optical magnitudes in the $U$, $B$, and $R$ bands for about 300 of the stars.

## 2. OBSERVATIONS AND DATA REDUCTIONS

A description of the UIT instrument, including plots of the wavelength dependence of the sensitivity of the bandpasses, is found in Stecher et al. (1992). The wavelength centroids of the B1 and A1 bandpasses used in observing M31 are 1520 and 2490 Å, with bandwidths 354 and 1150 Å, respectively. Magnitudes in the two bands are referred to as $m_{152}$ and $m_{249}$. Figures 1–4 (Plates L1–L4) show the longest near-UV and far-UV exposures of the nuclear and southern disk fields of M31, with the boundaries of the van den Bergh associations indicated. The exposure numbers, bandpasses, and exposure times of the images used in this investigation are given in Table 1. The UIT data reduction process, including digitization, linearization, and flat-fielding, is detailed in Stecher et al. (1992). The absolute calibration is determined as the ratio of the mean flux over the UIT bandpass from well-exposed *IUE* spectra of several stars imaged by UIT during the *Astro 1* mission to the total image fluxes in instrumental units above sky in a 15 pixel (17″) radius aperture, which is large enough to contain all the stellar signal. The uncertainty in the resulting calibration is estimated to be $\sim 10\%$ relative to *IUE* and 15% overall.

## 3. ANALYSIS

Stars are located, and aperture and point-spread function (PSF) fit photometry is performed using IDL implementations

[1] Hughes STX, 4400 Forbes Blvd, Lanham, MD 20706.
[2] Space Telescope Science Institute, Homewood Campus, Baltimore, MD 21218.
[3] University of Virginia, P.O. Box 3818, Charlottesville, VA 22903.
[4] National Radio Astronomy Observatory, Edgemont Rd., Charlottesville, VA 22903.
[5] Laboratory for Astronomy and Solar Physics, NASA/GSFC, Greenbelt, MD 20771.

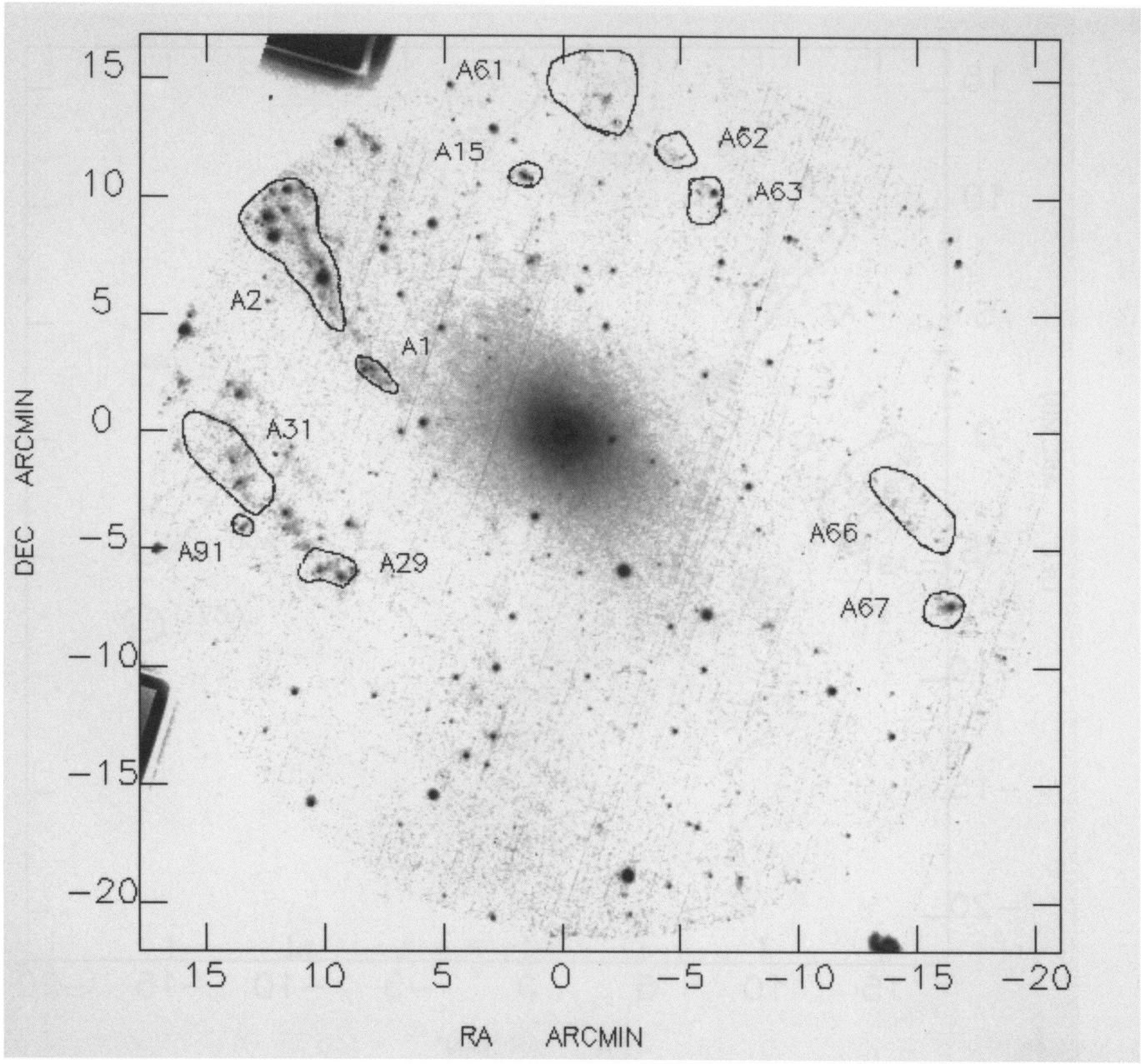


FIG. 1.—UIT A1 band image NUV0324, centered on the nucleus of M31. Van den Bergh (1964) OB associations are enclosed, and numbered.

HILL et al. (see 414, L9)

PLATE L2

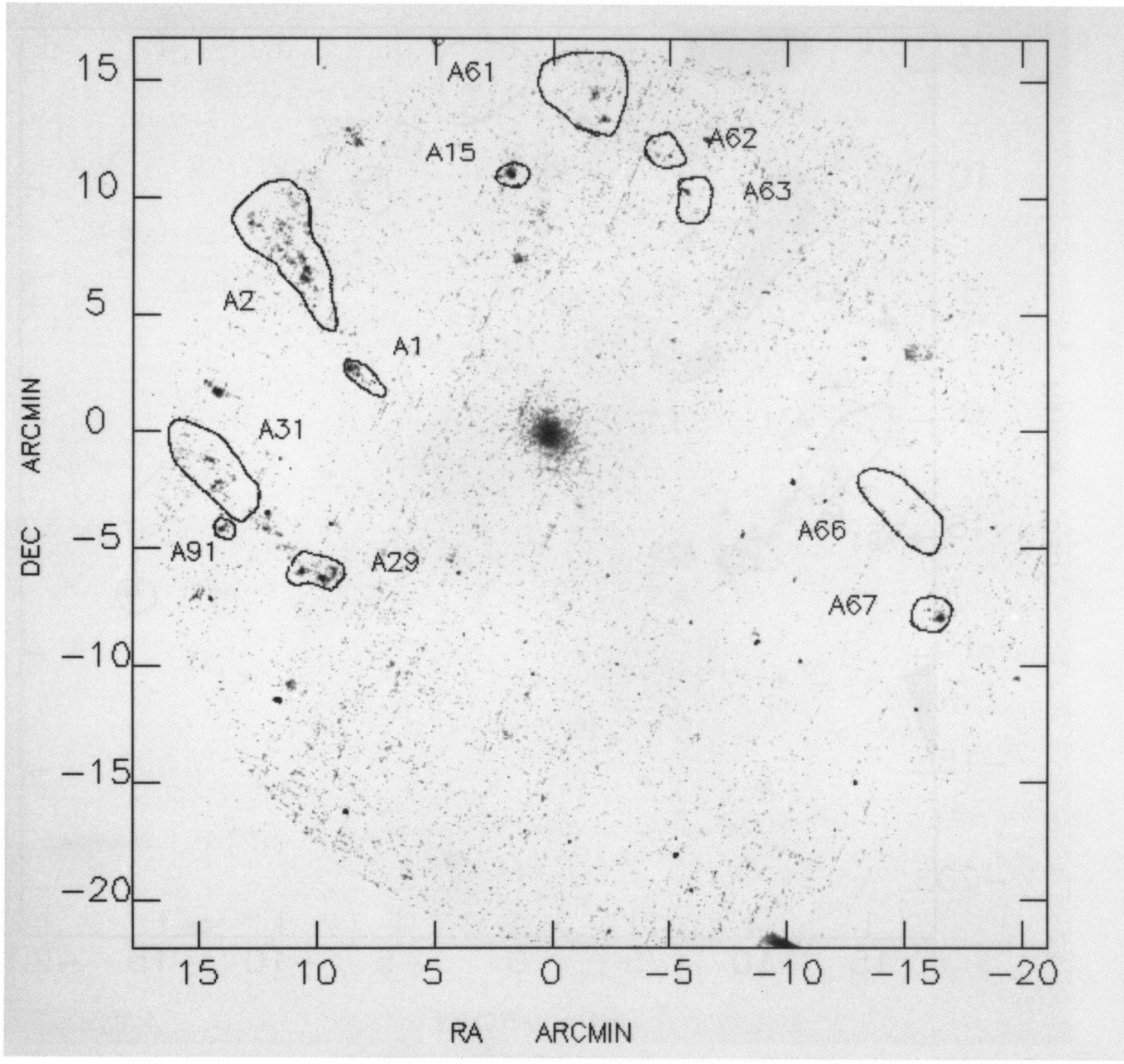


FIG. 2.—UIT B1 band image FUV0266, centered on the nucleus of M31, and registered with Fig. 1

HILL et al. (see 414, L9)

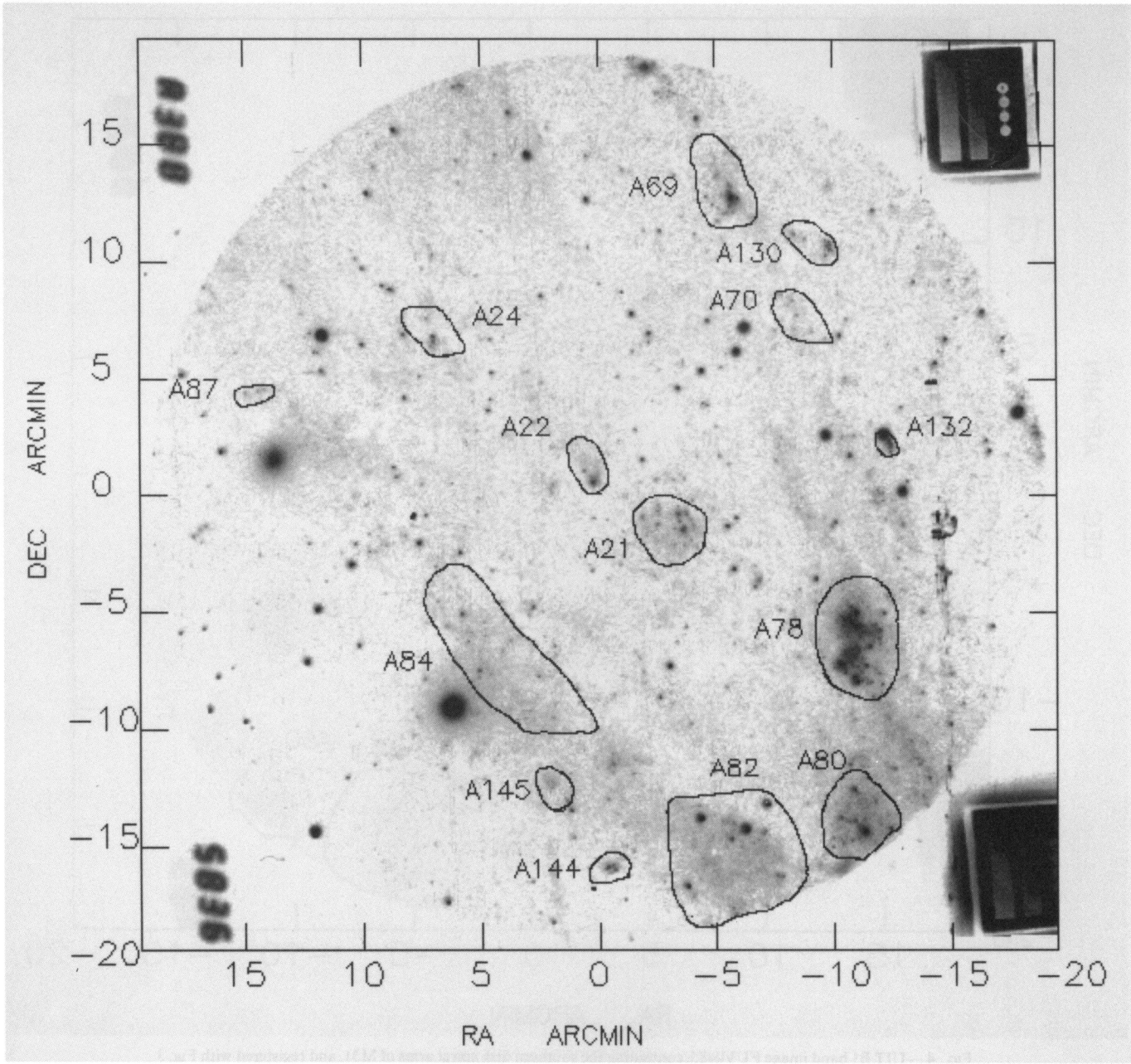


FIG. 3.—UIT A1 band image NUV0388, containing the southern disk spiral arms of M31 and the companion galaxy M32

HILL et al. (see 414, L9)

PLATE L4

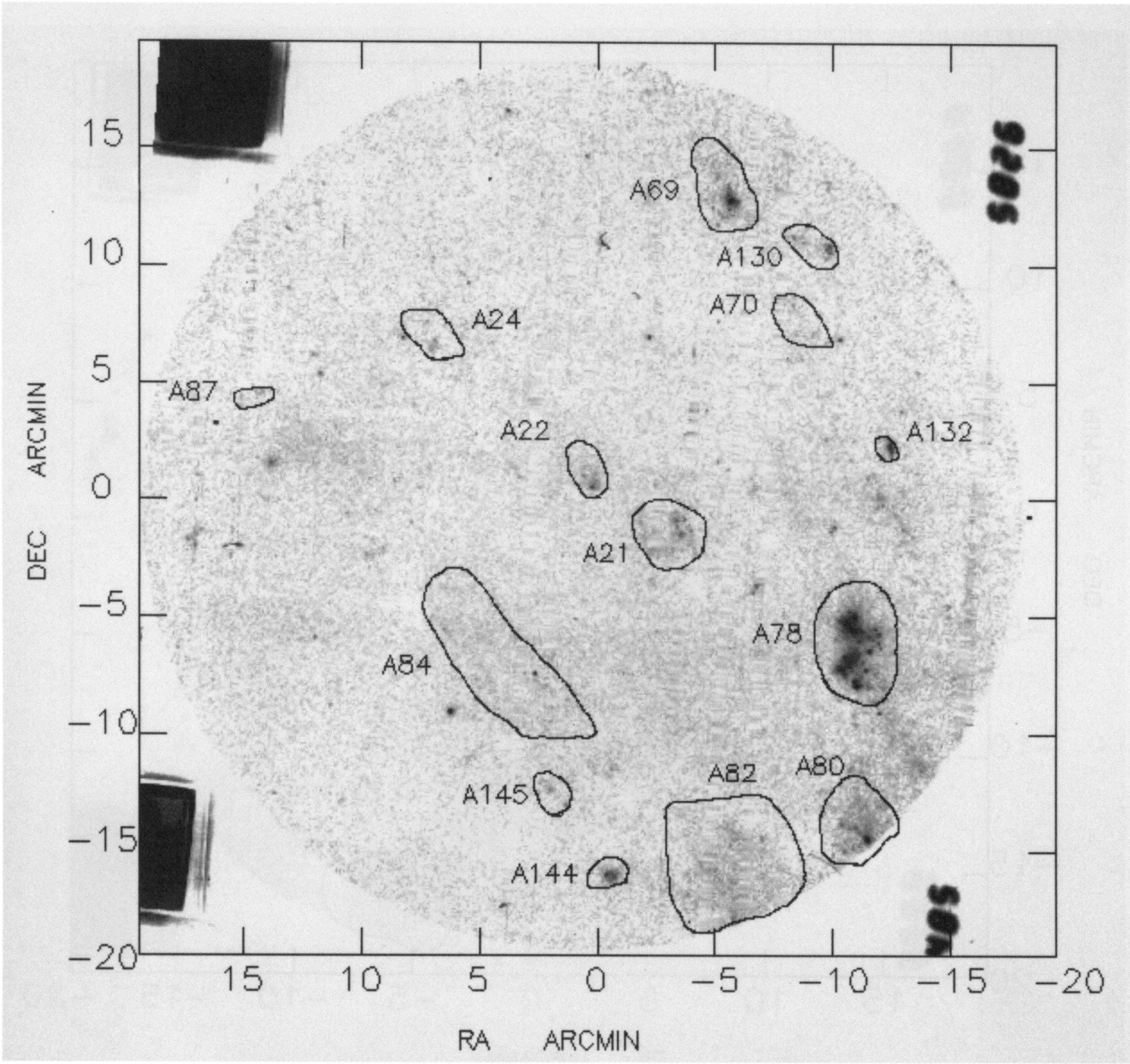


FIG. 4.—UIT B1 band image FUV0485, containing the southern disk spiral arms of M31, and registered with Fig. 3

HILL et al. (see 414, L9)

TABLE 1

UIT IMAGES USED

| Field | UIT Bandpass | UIT Image Number | Exposure Time (s) |
|---|---|---|---|
| M31 | B1 | FUV0266 | 384 |
| M31 | A1 | NUV0236 | 330 |
| M32-N206 | B1 | FUV0485 | 582 |
| M32-N206 | A1 | NUV0388 | 583 |

of DAOPHOT algorithms (Stetson 1987). We identify 76 stellar sources in OB associations on both the near-UV and far-UV images in addition to the 30 stars in NGC 206 reported earlier (Hill et al. 1992b).

Aperture photometry is done with apertures of radius 3 pixels (3".4). PSF-fit photometry uses point-spread functions constructed for each bandpass from a few bright isolated stars. Aperture corrections are determined separately for the nuclear field and the disk field images, from the profiles of bright isolated stars. Magnitudes $m_{152}$ are related to fluxes $f_{152}$ by $m_{152} = -2.5 \times \log(f_{152}) - 21.1$. The aperture corrected PSF-fit values of $m_{152}$ range from about 14 to 18. A total of 76 stars are measured in the 24 van den Bergh (1964) associations numbered 1, 2, 15, 21, 22, 24, 29, 31, 61, 62, 63, 66, 67, 69, 70, 80, 82, 84, 87, 91, 130, 132, 144, and 145. Other than NGC 206 (A78), the largest number of stars (15) is measured in A21.

Figure 5*a* is the $m_{152}$, $m_{152} - m_{249}$ color-magnitude diagram (CMD) for the stars which are members of associations other than NGC 206. Figure 5*b* is the CMD for the stars in NGC 206. The range and distribution of the $m_{152}$ magnitudes in the two plots is quite different. Eight of the 30 stars measured in NGC 206 (26%) are brighter than $m_{152} = 15.2$, while only three of the 76 stars measured in other associations (3%) are brighter than that limit. The apparent lack of stars fainter than $m_{152} = 16.41$ in NGC 206 is probably caused by a plethora of faint stars, together with diffuse scattered light, producing an enhanced noisy background, which leads to a sensitivity limit $m_{152} \sim 16.5$ in this region. Reddening lines are shown on Figures 5*a* and 5*b*, which assume extinction in the UIT bands within M31 to follow the LMC reddening law (Hutchings, Massey, & Bianchi 1987; Hutchings et al. 1992).

We estimate the extinction for each association, except NGC 206, using the relation between $E(B-V)$ and distance from the nucleus in the plane of M31 determined by Hodge & Lee (1988) in their CCD photometric investigation of five fields in M31. Unfortunately none of the associations discussed here is in any of fields they observe. The extinction in NGC 206 is assumed to be described by the reddening model for the star MAC 277 proposed by Hutchings et al. (1987), which incorporates $E(B-V) = 0.11$ of Galactic foreground extinction and $E(B-V) = 0.10$ of local M31 extinction, following the LMC extinction curve (Fitzpatrick 1985). The extinction so determined for NGC 206 is only about 0.60 of that given by the Hodge & Lee (1988) relation, consistent with the minimum in H I column density found there (Brinks & Bajaja 1986). For the other associations we assume a Galactic foreground extinction of 0.08, with the remainder described by the LMC extinction curve. The present analysis would benefit greatly from an increase in the number of M31 stars with accurate UV and optical extinction measurements. More spectral types, together with optical and UV photometry, would be required.

Maximum ages for the most recent episode of star formation are estimated for each association assuming the star with the brightest far-UV magnitude to be a blue supergiant with maximum far-UV luminosity. The evolutionary tracks of Schaller et al. (1992) for stars of mass 12, 15, 20, 25, 40, 60, 85, and 120 $M_\odot$ are then used to estimate the mass and age under this assumption. The resulting masses are lower limits, while the age is an upper limit. Upper limits to the mass are derived assuming the brightest star to be on the zero-age main sequence. This method of determining the age is similar to that employed by Regan & Wilson (1993), in their study of M33 associations. In estimating the masses and ages, we assume that the brightest star we measure in each association is a

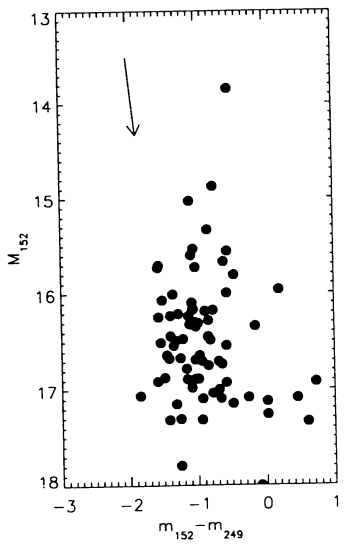


FIG. 5*a*

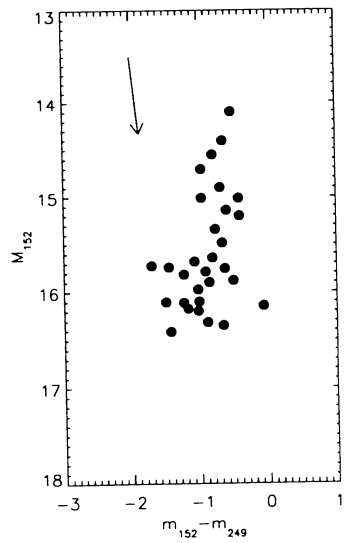


FIG. 5*b*

FIG. 5.—(*a*) $m_{152}$ vs. $m_{152} - m_{249}$ for stars not within NGC 206. The reddening arrow shows the relative effects on $m_{152}$ and $m_{152} - m_{249}$ of additional extinction with the LMC reddening curve. (*b*) $m_{152}$ vs. $m_{152} - m_{249}$ for stars in NGC 206. The reddening arrow shows the relative effects on $m_{152}$ and $m_{152} - m_{249}$ of additional extinction with the LMC reddening curve.

single star. We have determined absolute magnitudes in the UIT bands assuming a distance modulus of 24.26 (Welch et al. 1986), which is probably in error by less than 0.2 mag.

The evolutionary models of Schaller et al. (1992), together with the model atmospheres of Kurucz (1992), are used to determine the relation between the brightest $m_{152}$, stellar mass, and age. Table 2 gives the van den Bergh (1964) association number, the number of stars measured in both far-UV and near-UV bands, the brightest far-UV magnitude, the UV color of the brightest star, the adopted far-UV extinction, the estimated age, the mass of the brightest star assuming it to be a supergiant, and the mass of the brightest star assuming it to be a dwarf, for all 24 associations plus NGC 206. We estimate lower limits to the maximum stellar mass at $\sim$60–100 $M_\odot$ in NGC 206, A29, A61, A63, A130, and A132. The limits are in the range $\sim$20–56 $M_\odot$ in A1, A2, A15, A21, A22, A24, A31, A62, A66, A67, A69, A70, A80, A82, A84, A87, A91, A144, and A145.

The brightest of the 76 brightest association member UV sources coincides with Hodge cluster 205 in association A69 (Hodge 1979) and is probably multiple. The chart showing A69 in *The Atlas of the Andromeda Galaxy* (Hodge 1981) shows cluster 205 as a tight grouping of 4–5 bright stars. The age and maximum stellar mass for A69 were estimated using the brightest association star outside cluster 205.

Assuming UV extinctions determined as discussed above, together with distance modulus 24.26, we obtain the dereddened absolute CMD of Figure 6 for associations A21 and NGC 206. The evolutionary tracks of Schaller et al. (1992) for 20, 40, and 60 $M_\odot$ stars are also shown in Figure 6. The early redward evolution is shown as solid lines, while the later evolution back to the blue is shown for 40 and 60 $M_\odot$ as dotted lines. In these cases, most of the stellar lifetime is spent in evolution to the red. Figure 6 suggests that the maximum mass

TABLE 2

ASSOCIATIONS, NUMBER OF MEASURED STARS, PHOTOMETRY OF BRIGHT, FAINT STARS

| vdB | $N_{stars}$ | $m^1_{152}$ | $(m_{152}-m_{249})^1$ | $A_{152}$ | Age (Myr) | $M_{SG}$ ($M_\odot$) | $M_{MS}$ ($M_\odot$) |
|---|---|---|---|---|---|---|---|
| 1.... | 5 | 15.97 | 0.20 | 1.9 | 6.1 | 27 | 59 |
| 2.... | 4 | 16.92 | −0.48 | 1.9 | 8.8 | 19 | 34 |
| 15.... | 3 | 14.87 | −0.75 | 1.9 | 4.1 | 46 | 118 |
| 21.... | 15 | 16.17 | −0.77 | 2.7 | 4.9 | 36 | 85 |
| 22.... | 2 | 15.56 | −0.56 | 2.7 | 4.0 | 48 | >120 |
| 24.... | 3 | 16.34 | −1.45 | 2.7 | 5.2 | 34 | 77 |
| 29.... | 5 | 15.03 | −1.10 | 3.4 | 2.7 | 98 | >120 |
| 31.... | 3 | 16.00 | −0.56 | 2.9 | 4.2 | 43 | 109 |
| 61.... | 2 | 15.60 | −1.09 | 3.5 | 3.2 | 70 | >120 |
| 62.... | 1 | 16.31 | −0.99 | 3.8 | 3.6 | 56 | >120 |
| 63.... | 1 | 16.01 | −1.36 | 3.8 | 3.3 | 65 | >120 |
| 66.... | 1 | 17.04 | −0.78 | 3.5 | 5.0 | 35 | 81 |
| 67.... | 2 | 15.67 | −0.61 | 3.1 | 3.7 | 54 | >120 |
| 69.... | 8 | 15.81 | −0.46 | 3.1 | 3.8 | 51 | >120 |
| 70.... | 2 | 16.51 | −1.54 | 3.5 | 4.1 | 45 | 115 |
| 78.... | 30 | 14.10 | −0.53 | 1.8 | 3.4 | 61 | >120 |
| 80.... | 1 | 16.71 | −0.69 | 3.4 | 4.5 | 39 | 95 |
| 82.... | 2 | 17.79 | −0.08 | 2.4 | 10.9 | 16 | 28 |
| 84.... | 2 | 16.89 | −1.15 | 2.4 | 7.1 | 23 | 46 |
| 87.... | 1 | 16.88 | −1.48 | 2.4 | 7.1 | 23 | 46 |
| 91.... | 1 | 16.30 | −1.03 | 2.4 | 5.7 | 30 | 66 |
| 130.... | 6 | 16.10 | −1.08 | 3.8 | 3.4 | 61 | >120 |
| 132.... | 3 | 15.53 | −1.05 | 3.8 | 2.8 | 90 | >120 |
| 144.... | 2 | 15.71 | −1.57 | 1.7 | 6.0 | 28 | 61 |
| 145.... | 1 | 16.54 | −1.35 | 1.7 | 8.2 | 20 | 37 |

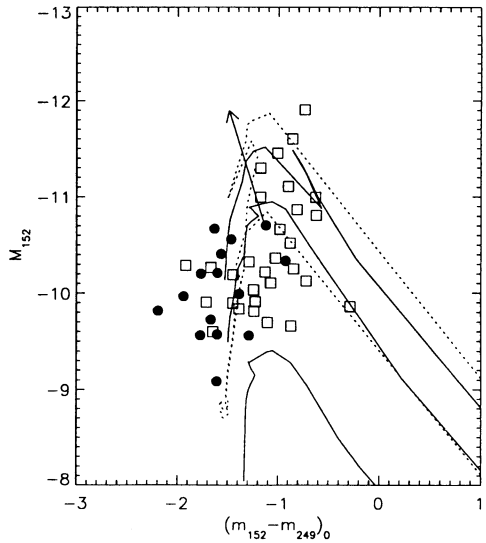


FIG. 6.—Dereddened, absolute CMD $M_{152}$ vs. $(m_{152}-m_{249})_0$. Absolute magnitudes computed assuming $m - M = 24.26$. Stars in NGC 206 are shown as open squares. Stars in A21 are shown as solid circles. Dereddening is performed assuming $A_{152} = 1.8$ mag and $A_{249} = 1.6$ mag, for NGC 206, while $A_{152} = 2.7$ mag and $A_{249} = 2.3$ mag for A21. Evolutionary tracks from Schaller et al. (1992) for stars of mass 20, 40, and 60 $M_\odot$ shown as solid lines for early evolution to the red, while the later blueward evolution is shown as dotted lines for the 40 and 60 $M_\odot$ models. The arrow shows the effect of dereddening A21 magnitudes and colors by the additional amount necessary to give equal $m_{152}$ for the brightest stars.

of the A21 stars is about 40 $M_\odot$, if the brightest stars are supergiants. On the other hand, Figure 6 suggests that stellar masses in NGC 206 are as high as $\sim$60 $M_\odot$. The apparently larger upper mass limit in NGC 206 suggests that either the extinction in A21 has been underestimated, the initial mass function (IMF) is different in A21 than in NGC 206, or that NGC 206 has at least some younger massive stars. The UV colors of the two extremely blue stars in the CMDs of A21 and NGC 206 are probably due to errors in PSF fitting, since the colors of these stars from aperture photometry are 0.3–0.4 mag redder.

Increasing the reddening correction of stars in A21 by 1.2 mag to give approximately equal $m_{152}$ for the brightest stars in A21 and NGC 206 gives corrected $m_{152} - m_{249}$ colors bluer by 0.2 mag. Such colors are bluer than those of NGC 206 stars of similar corrected $M_{152}$ by about 0.6 mag, as shown by the arrow in Figure 6. So, an underestimated extinction for A21 is probably not the explanation for the brightest star being fainter there. The difference between the lifetime of a 60 $M_\odot$ star and a 40 $M_\odot$ star is about 2–3 Myr, according to the evolutionary models of Schaller et al. (1992). We attribute the presence of brighter stars in NGC 206 to a younger age for the most recent star formation. Hodge (1992) suggests that the variation observed in the optical magnitudes of the brightest members of M31 OB associations is primarily an age effect.

UIT $m_{152}$ magnitudes brighter than 18.0 exist for 106 stars in the part of M31 imaged during the *Astro 1* mission. We estimate that $\sim$70 more stars would be detected in the northern spiral arms not observed by UIT, giving $\sim$180 altogether. On the other hand, approximately 500 stars brighter than $m_{152} = 17.0$ have been measured on a UIT far-UV image of M33, a smaller galaxy of later type with similar distance. We conclude that M31 is currently forming stars at a low rate compared with galaxies of later type. M31's star formation rate

has already been determined to be significantly lower than the Galactic rate by several authors (e.g., van den Bergh 1964; Walterbos 1988; Dopita 1987).

We gratefully acknowledge the contributions made by the hundreds of people involved in the *Astro 1* mission, including the many officials at NASA headquarters whose support brought it through a long and difficult gestation period. Funding for the UIT project has been through the Spacelab Office at NASA headquarters under Project number 440-51. R. W. O. gratefully acknowledges NASA support of portions of this research through grants NAG5-700 and NAGW-2596 to the University of Virginia.

REFERENCES

Bohlin, R. C., Cornett, R. H., Hill, J. K., O'Connell, R. W., & Stecher, T. P. 1990, ApJ, 352, 55
Brinks, E., & Bajaja, E. 1986, A&AS, 169, 14
Dopita, M. 1987, in Star Forming Regions, ed. M. Peimbert & J. Jukaju (Dordrecht: Reidel), 501
Fitzpatrick, E. L. 1985, ApJ, 299, 219
Hill, J. K., et al. 1992a, ApJ, 395, L37
Hill, J. K. Bohlin, R. C., & Stecher, T. P. 1984, ApJ, 277, 542
Hill, J. K., Isensee, J. I., Bohlin, R. C., O'Connell, R. W., Roberts, M. S., Smith, A. M., & Stecher, T. P. 1993, in preparation
Hill, J. K., et al. 1992b, ApJ, 395, L33
Hodge, P. 1979, AJ, 84, 744
———. 1981, Atlas of the Andromeda Galaxy (Seattle: Univ. Washington Press)
———. 1992, The Andromeda Galaxy (Dordrecht: Kluwer)
Hodge, P., & Lee, M. G. 1988, ApJ, 329, 651
Hodge, P., Mateo, M., Lee, M., & Geisler, D. 1987, PASP, 99, 173
Hutchings, J. B., Bianchi, L., Lamers, H. J. G. L. M., Massey, P., & Morris, S. C. 1992, ApJ, 400, L35
Hutchings, J. B., Massey, P., & Bianchi, L. 1987, ApJ, 322, L79
Kurucz, R. L. 1992, in The Stellar Populations of Galaxies, ed. B. Barbuy & A. Renzini (Dordrecht: Kluwer), 225
Massey, P., Armandroff, T. E., & Conti, P. S. 1986, AJ, 92, 1303
Regan, M. W., & Wilson, C. D. 1993, AJ, 105, 499
Schaller, G., Schaerer, D., Meynet, G., & Maeder, A. 1992, A&AS, 96, 269
Stecher, T. P., et al. 1992, ApJ, 395, L1
Stetson, P. B. 1987, PASP, 99, 101
van den Bergh, S. 1964, ApJS, 9, 65
Walterbos, R. 1988, in Galactic and Extragalactic Star Formation, ed. R. E. Pudritz & M. Fich (Dordrecht: Kluwer), 361
Welch, D., McAlary, C., McLaren, R., & Madore, B. 1986, ApJ, 305, 583